New constraints on the Δ production cross section

J. Cugnon,[1,*] S. Leray,[1,2] E. Martinez,[3] Y. Patin,[3] and S. Vuillier[1]
[1]*CEA DAPNIA, CE Saclay, F-91191 Gif-sur-Yvette Cedex, France*
[2]*LNS, CE Saclay, F-91191 Gif-sur-Yvette Cedex, France*
[3]*DPTA/SPN, CEA, Boîte Postale 12, F-91680 Bruyères-le-Châtel, France*
(Received 30 September 1996; revised manuscript received 25 June 1997)

Recent measurements of proton spectra issued from neutron beam interactions with a hydrogen target in the 0.2−1.6 GeV range are exploited to perform a new analysis of the bulk of the available appropriate data and to extract from the latter the Δ-production cross section and related parameters. Among these, the slope parameter of the angular distribution is accurately determined and shown to be close to the slope parameter for pp elastic scattering for incident momentum larger than approximately 1.4 GeV/c. Constraints introduced by isospin conservation are also briefly discussed. [S0556-2813(97)06211-0]

PACS number(s): 13.75.Cs, 14.20.Gk, 25.40.Sc

I. INTRODUCTION

Proton-nucleus as well as heavy ion collisions in the GeV/nucleon range are generally analyzed in terms of transport models (see for instance Refs. [1,2]). The latter require a good knowledge of the elementary elastic and inelastic cross sections. The nucleon-nucleon elastic and inelastic cross sections are rather well documented [3–6]. Above the inelastic threshold, the main inelastic channel, namely one pion production, is largely dominated by the intermediate excitation of the Δ resonance. The lifetime of the latter being sometimes of the same order of the time separation between successive hadron-hadron collisions (in a complex collision process), it is necessary to explicitly take account of the Δ degrees of freedom. In the simplest (classical) description, the knowledge of the cross sections for processes involving Δ resonances is required. For some cases, like the $N\Delta \rightarrow N\Delta$ scattering,[1] the information can be obtained from model calculations only. For other cases, like the $NN \rightarrow N\Delta$ production process, the cross section can be inferred from experimental data. Unfortunately, for this particular case, only a limited amount of data is available [3,6–8]. The recent measurements [9] of small angle proton spectra in np collisions in the 0.2−1.6 GeV range offer an opportunity to gain more information about the $np \rightarrow N\Delta$ reaction parameters. The purpose of this paper is to reanalyze the bulk of the existing data including these new measurements in order to improve the knowledge of the $NN \rightarrow N\Delta$ cross section, of the angular distribution of the produced Δ's, and of related parameters. The paper is divided as follows. Section II makes a brief survey of the aspects of the experimental method used in Ref. [9] that are relevant for our purpose. Section III describes the parametrization of the elastic and inelastic contributions adopted in this work and the motivation for this choice. Section IV gives the results yielded by our global analysis of the data. Finally, Sec. V is devoted to the discussion of the results and of the implications of the latter for the calculations of the proton-nucleus collisions in the GeV range.

II. THE NEUTRON-PROTON MEASUREMENTS AT SATURNE

The data consist of proton recoil spectra issued from the interaction of quasi-monoenergetic neutron beams with a liquid hydrogen target. Momentum evaluation and identification of protons are made using a magnetic spectrometer. Details of the experimental technique and full presentation of the data are given elsewhere [9] (the data shown in the figures below can be considered as a very partial account of the results described in Ref. [9]). Neutron beams are obtained from deuteron stripping on a Be target [10] from 0.1 to 1.15 GeV/nucleon and from ^{3}He breakup from 1.15 to 1.6 GeV/nucleon. The consistency of the two methods has been checked [9]. The neutron beam energy is spread by neutron Fermi motion inside the incident composite particle. The neutron beam profile is evaluated from the measured proton spectra considering the width (FWHM) of the elastic peak as the quadratic sum of the spectrometer resolution (3%) and the incident neutron dispersion. This procedure is justified at least by the presence of a well-defined elastic proton peak (without any tail) under the inelastic threshold for the case of incident deuterons. For the case of incident ^{3}He particles, such a direct check has not been done. However, the detailed analysis of Ref. [9] shows that the neutron beam is largely monoenergetic, corresponding to a Gaussian shape, except perhaps for the highest ^{3}He energy, where a tail of a few percent might exist. Let us notice that in the energy range under study in this paper, the considered obversables are smoothly varying with energy and the possible small tail component of the beam is not expected to influence our analysis. The calculated values of the FWHM of the neutron beam profile are presented in Table I. The neutron beam intensity has been determined by using the elastic cross section of Ref. [11]. To ensure a proton detection efficiency of 100%, a cut is applied at 3° or 5.5° to the proton emission angle. The background created by the windows of the hydrogen target, which represents 5 to 15% of the detected yields,

*On leave of absence from University of Liège, Physics Department, B5, B-4000 Sart Tilman Liège 1, Belgium.

[1]N stands generically for n or p.

 © 1997 The American Physical Society

TABLE I. Calculated FWHM of energy distribution of neutrons produced by d and ^{3}He breakup on a Be target.

			$d+$Be			
d momentum (MeV/c)	645	955	1219	1464	1696	1866
FWHM (MeV/c)	57.74	65.50	75.31	85.92	96.80	105.08
			^{3}He$+$Be			
^{3}He momentum (MeV/c)		1866	2033	2142	2251	2359
FWHM (MeV/c)		170.08	178.23	183.60	188.78	193.84

has been measured and systematically subtracted from the measured proton spectra.

III. DETERMINATION OF THE Δ PRODUCTION CROSS SECTION

A. Basic formulas

We start with the inclusive $np\to p+X$ cross section (similar considerations can be made for any of the $NN\to N+X$ cross sections). In the energy range covered by the experiment of Ref. [9], we decompose it into three components:

$$\frac{d\sigma}{d\Omega dp}=\left(\frac{d\sigma}{d\Omega dp}\right)_{\rm el}+\left(\frac{d\sigma}{d\Omega dp}\right)_{\Delta}+\left(\frac{d\sigma}{d\Omega dp}\right)_{\rm p.s.}, \quad (3.1)$$

corresponding to the elastic scattering, Δ production and ''direct'' (phase space) pion production, respectively. We adopt here a semiclassical picture of pion production: production of Δ particles with a definite mass and no interference between direct and resonant pion production. We will comment on this point below. The first term in Eq. (3.1) can be written, in the c.m. frame, as

$$\left(\frac{d\sigma}{d\Omega dp}\right)_{\rm el}=\delta(p-p_{\rm c.m.})\sigma_{\rm el}A\{e^{B_{np}t}+ae^{B_{np}u}+ce^{\alpha_c u}\}, \quad (3.2)$$

where $p_{\rm c.m.}$ is the neutron (or proton) c.m. momentum, $\sigma_{\rm el}$ is the elastic neutron-proton cross section and the curly bracket gives the angular distribution in terms of the Mandelstam variables t and u. The latter quantities are related to the polar angle θ_p of the outgoing proton (relative to the direction of the incident neutron) by

$$t=-2p^2_{\rm c.m.}(\cos\theta_p+1), \quad u=2p^2_{\rm c.m.}(\cos\theta_p-1). \quad (3.3)$$

The parameter A is fixed by normalization, as the angular integration of Eq. (3.2) should give $\sigma_{\rm el}$. In the following, the latter is taken from the systematics of Ref. [6]. In the energy range under study, it differs from the values given in Ref. [11] by 2 to 3% at the most. A careful analysis of the np available elastic data [12–20] in the 0.3-1.6 GeV incident energy range has allowed to determine the parameters B_{np}, α_c, a and c rather accurately . The parameter α_c turns out to be close to 100 $(\text{GeV}/c)^{-2}$. The incident momentum dependence of the other parameters is shown in Fig. 1. They can be parameterized as

$$\begin{aligned} B_{np}&=9.87-4.88p_{\rm lab}, \quad p_{\rm lab}<1.1 \ \text{GeV}/c \\ &=3.68+0.76p_{\rm lab}, \quad p_{\rm lab}>1.1 \ \text{GeV}/c, \end{aligned}$$

$$a=\left(\frac{0.8}{p_{\rm lab}}\right)^2, \quad (3.4)$$

$$\begin{aligned} c&=6.23\exp(-1.78p_{\rm lab}), \quad p_{\rm lab}<1.7 \ \text{GeV}/c \\ &=0.3, \quad p_{\rm lab}>1.7 \ \text{GeV}/c. \end{aligned}$$

In these relations, $p_{\rm lab}$ should be expressed in GeV/c and B_{np} is given in $(\text{GeV}/c)^{-2}$. The piecewise linear dependence of B_{np} (with $p_{\rm lab}$), though largely sufficient, has been adopted for simplicity. It is responsible for the change of slope in the dashed curve of Fig. 1. The third term in the curly bracket of Eq. (3.2) accounts for the rapid rise of the cross section at very backward angles, which is due to the charged pion exchange process [21,15]. For $p_{\rm lab}<0.8$ GeV/c, where the angular distribution is largely symmetric and more isotropic, we used the same parametrization (with a polynomial of fourth degree in $\cos\theta$) as in Ref. [22].

The second term in Eq. (3.1) stands for the protons emitted, either directly in the $np\to p\Delta^0$ process or indirectly in the Δ decay following the $np\to p\Delta^0$ and $np\to n\Delta^+$ reactions. In order to write down this contribution we param-

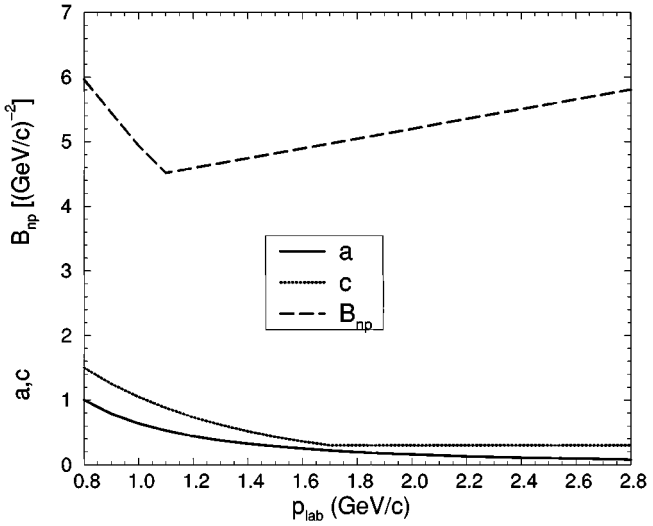

FIG. 1. Incident momentum dependence of the parameters [Eq. (3.2)] describing the angular distribution in elastic pn scattering.

etrize the $np \to p\Delta^0$ cross section as follows. Let $f(m_\Delta)$ be the probability density for the creation of a Δ particle of mass m_Δ. We then write

$$\frac{d\sigma}{d\Omega_\Delta dm_\Delta dp_\Delta} = \sigma_{np\to p\Delta^0} f(m_\Delta) B(e^{B_{\rm in}t} + e^{B_{\rm in}(t_1-t)}) \times \frac{p_\Delta^{\rm c.m.} p_{\rm in}^{\rm c.m.}}{\pi} \delta(p_\Delta - p_\Delta^{\rm c.m.}), \tag{3.5}$$

where $p_\Delta^{\rm c.m.}$ is the c.m. momentum of the Δ particle with mass m_Δ and $p_{\rm in}^{\rm c.m.}$ is the incident neutron c.m. momentum. The mass distribution function is taken proportional to the pion-nucleon cross section

$$f(m_\Delta) = F_N \frac{q^3}{q^3 + (0.18)^3} \frac{1}{1 + 4\left(\frac{m_\Delta - 1.215}{0.130}\right)^2}, \tag{3.6}$$

with

$$q = \frac{\sqrt{[m_\Delta^2 - (m_N + m_\pi)^2][m_\Delta^2 - (m_N - m_\pi)^2]}}{2m_\Delta}, \tag{3.7}$$

where m_N and m_π are respectively the nucleon mass and the pion mass. In Eq. (3.6), q and m_Δ should be expressed in GeV/c and GeV, respectively, and F_N is a normalization constant determined by

$$\int_{m_\Delta^i}^{m_\Delta^s} f(m_\Delta) dm_\Delta = 1, \tag{3.8}$$

where $m_\Delta^i = m_N + m_\pi$ and m_Δ^s is the maximum value of m_Δ allowed by energy conservation, i.e., $\sqrt{s} - m_N$, $\sqrt{s}$ being the np c.m. energy. The quantity B in Eq. (3.5) is a normalization constant (determined by the fact that integrating over all variables the r.h.s. should give $\sigma_{np\to p\Delta^0}$). It is given by

$$B = \frac{B_{\rm in}}{2} e^{B_{\rm in}(t_0 - t_1)}, \tag{3.9}$$

where t_0 and t_1 are the maximum and minimum values of the Mandelstam variable $t = (p_\Delta - p_n)^2$. An expression similar to Eq. (3.5) holds for the $np \to n\Delta^+$ process. From these expressions, we write the second term in Eq. (3.1) as

$$\left(\frac{d\sigma}{d\Omega dp}\right)_\Delta = \int dm_\Delta \left(\frac{d\sigma}{d\Omega_\Delta dm_\Delta dp_\Delta}\right)_{\theta_p = \pi - \theta_\Delta, p = p_\Delta} + \sum_{\Delta = \Delta^0, \Delta^+} \left(\frac{d\sigma}{d\Omega_\Delta dm_\Delta dp_\Delta}\right) \left(\frac{\partial(\Omega_\Delta, p_\Delta)}{\partial(\Omega, p)}\right), \tag{3.10}$$

where we have introduced the Jacobian corresponding to the ''transformation'' of the Δ parameters Ω_Δ, p_Δ to those of the produced proton Ω, p through the Δ decay. The latter can be evaluated from the following model for Δ decay. The helicity λ of the Δ particle is supposed to be equal to $\cos^2\theta$, where θ is the c.m. polar angle at which it is produced. The angular distribution of the produced pions (or of the emitted nucleons) is taken as due to a p-wave decay

$$\frac{d\sigma}{d\Omega} = 1 + 3\lambda \cos^2\theta_\pi, \tag{3.11}$$

where θ_π is the angle between the pion direction and the Δ direction in the rest frame of the latter.

The last contribution in Eq. (3.1) can be written as

$$\left(\frac{d\sigma}{d\Omega dp}\right)_{\rm p.s.} = \sigma_{\rm p.s.}^{\rm inel} N e^{-\alpha p_\perp} \int \frac{d^3p_2}{(2\pi)^3} \int \frac{d^3p_\pi}{(2\pi)^3} \times \delta(\vec{p} + \vec{p}_2 + \vec{p}_\pi) \delta(\epsilon + \epsilon_2 + \epsilon_\pi - \sqrt{s}), \tag{3.12}$$

with obvious notation, N being a normalization constant determined by the fact that integrating over $\vec{p}$ should give $\sigma_{\rm p.s.}^{\rm inel}$. Distribution (3.12) differs from the uniform phase space density model by the presence of the exponential factor, where $p_\perp$ is the proton transverse momentum. This factor is necessary for reproducing the results accurately. Note that this is in keeping with the peripheral nature of the one pion production model, which favors the production of the nonresonant (pion + nucleon 2) production along the longitudinal direction.

Parametrizations (3.5)–(3.12) rest on a semiclassical picture of the pion production process. They indeed imply on-shell Δ-particles with definite mass and helicity. They can be viewed as a practical way to describe the measurements or even as a convenient formulation allowing a tractable treatment of the Δ degrees of freedom in transport models. They nevertheless retain the basic features of the $np \to NN\pi$ cross sections as calculated in the one pion exchange model [8,23]: the resonant (nonsymmetrical) shape centered around m_Δ in the dependence upon the pion-nucleon energy variable, the exponential t dependence and the symmetry between neutral pion and charged pion exchange, ensured through the symmetrized t dependence of Eq. (3.5). Of course, interference terms are neglected in this approach. According to Ref. [8], they are not important.

The parametric form of cross section (3.1) may look rather complicated. We want to stress however that the calculation of this quantity is straightforward by using simulation methods, as it is commonly done in transport models. We refer to Refs. [6,24] for a brief description of the methods.

B. Extraction of the $NN \to N\Delta$ cross section parameters

Having determined the elastic part of the $np \to p + X$ inclusive cross section, we performed a global fit of the inelasticity parameters, i.e., the same set of parameters $\sigma_{\rm p.s.}$, $\sigma_{np\to\Delta N}$, $B_{\rm in}$ and α is used to fit all kinds of data (proton, pion) irrespective of the emission angle. The parameters are allowed to vary with the neutron incident energy, except for α, as it turned out that a good fit is already obtained with a constant value. We did not attempt to reach a minimum χ^2 fit. As can be seen below, the quality of the fits is already very good and provides a parametrization of the cross sections of sufficient accuracy for being used as input in trans-

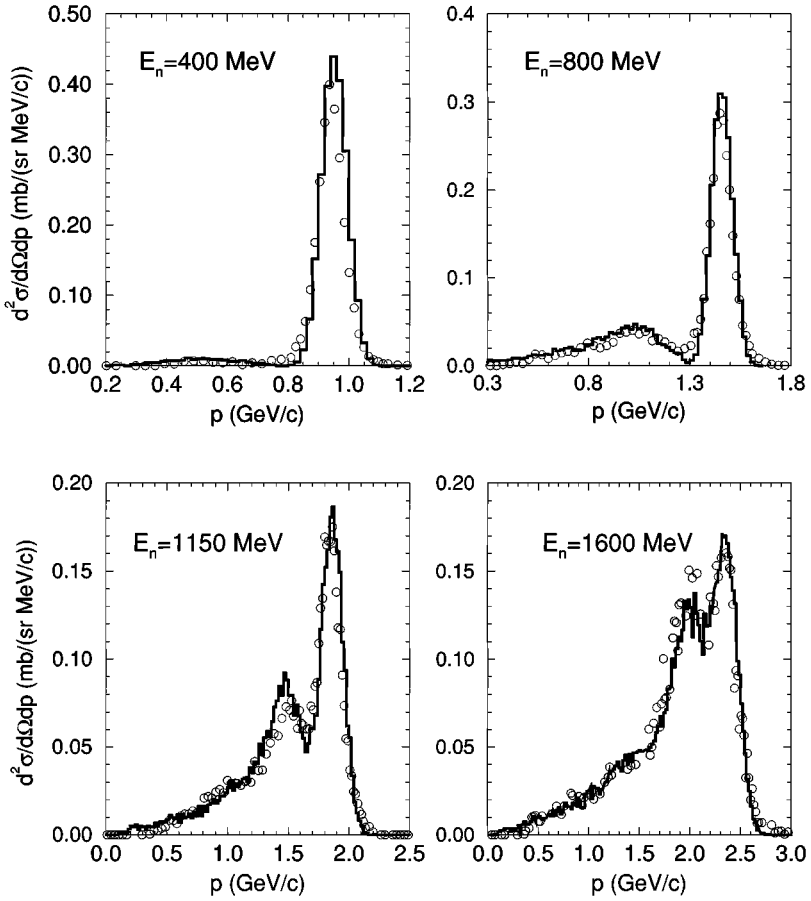

FIG. 2. Proton spectra integrated from 0 to 3° (circles) resulting from collisions of neutrons (of incident energy E_n) on a hydrogen target, compared to a fit using formula (3.1). The data (symbols) are taken from Ref. [9]. The experimental error bars are not shown, but are of the order of, or smaller than the size of the circles. The fit is given by the histograms and corresponds to the simulation of $\sim 10^6$ events.

port model calculations. In keeping with the usual procedure adopted in these calculations, we assume that the cross sections $\sigma_{np\to\Delta^0 p}$, $\sigma_{np\to\Delta^+ n}$ and $\sigma_{\text{p.s.}}$ sum up to the (relatively well-known) total inelastic cross section. In the energy range covered in this work, this seems largely reasonable (see the discussion in Sec. IV). The results of the fitting procedure are given in the next section.

IV. RESULTS

A. Analysis of the data

The data of Ref. [9] refer to proton spectra issued from interactions of a neutron beam at various energies extending from 0.2 to 1.6 GeV (0.644 to 2.358 GeV/c incident momentum, repectively) with a hydrogen target. They correspond to integration over polar angles from 0° to 3° and from 0° to 5.5°. The kind of agreement reached by the fitting procedure is given in Fig. 2. An equally good agreement is obtained for the data corresponding to the [0,5.5°] interval.

Before analyzing the effects of the ingredients of the parametrization, let us look at the various contributions of the inelastic part. They are given in Fig. 3 for $E_n = 0.8$ GeV ($p_{\text{lab}} = 1.463$ GeV/c). The most important contribution comes from the protons associated with a Δ^0 produced at backward c.m. angles. The protons then appear with a momentum of the order of 1 GeV/c. The protons associated with a Δ^0 emitted in the c.m. forward angles appear in the small bump around $p \approx 0.3$ GeV/c. Although the production is symmetric in the c.m., the height of this bump is much smaller than the one of the main peak because the same solid angle in the lab system corresponds in the c.m. system to different solid angles, in fact proportional to the square of the outgoing momenta. The protons issued from the decay of the Δ^0's and of the Δ^+'s appear as an almost structureless back-

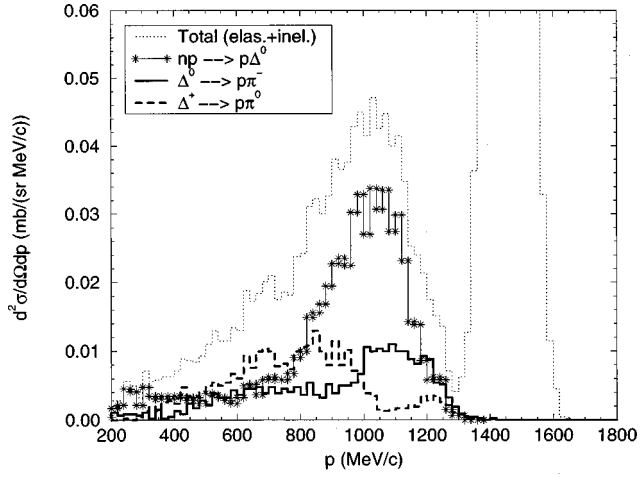

FIG. 3. Splitting of the inelastic part of the proton spectrum in various contributions, as indicated by Eq. (3.10) in np collisions at $E_n = 0.8$ GeV neutrons.

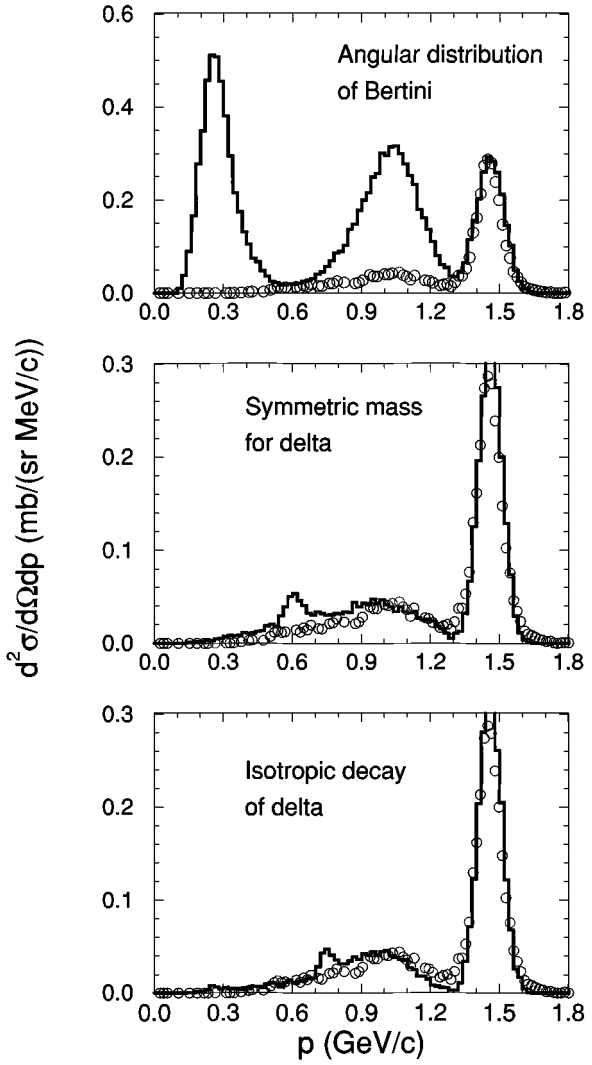

FIG. 4. Illustration of the importance of some of the ingredients of formula (3.10). The data are the same as those in the upper right corner of Fig. 2. The elastic contribution is the same for the three cases. The vertical scale has been changed to magnify the inelastic contribution in the central and lower part of the figure. See text for detail.

ground. The ''direct'' (phase space) production mechanism does not contribute at this energy.

The influence of several ingredients of the chosen parametrization are illustrated in Fig. 4. In the first part, the angular distribution proposed in Ref. [22] and used in many transport codes has been introduced. It differs from the bracket of Eq. (3.5) in the fact that the Δ particle production is limited to very forward angles. In the second part of the figure, a symmetric form of $f(m_\Delta)$, centered on 1.232 GeV, has been employed. Although the effect is not large (compared to Fig. 2), the fit is definitely better with expression (3.5). In the third part, the Δ's are supposed to decay isotropically in their rest frame. This modification, as well as the previous one, allows a more important production of protons in the ''middle'' of the available phase space, which is signalled by the small bump around $p=0.75$ GeV/c in Fig. 4(c). One can realize that the chosen parametrization form is well adapted to the data and should correspond rather well to the physical effects that have inspired our choice, even though the formulation is of classical nature.

A larger angular range can be tested using the data of Refs. [7,8]. The measurements are similar to those of Ref. [9], but the incident energy range extends from $E_n=0.74$ to 1.18 GeV ($p_{\rm lab}=1.39$ to 1.9 GeV/c) and the protons are detected at definite angles. Figure 5 gives the comparison for a few angles at $E_n=1.03$ GeV ($p_{\rm lab}=1.73$ GeV/c). Fits of similar or even better quality are achieved at the other energies.

We are mainly concerned here with np data, basically because there is no data of similar quality for the pp system, as far as we know. In order to test the decomposition (3.1) in this case, we however considered the data of Bugg *et al.* [25], who measured angle integrated nucleon spectra in coincidence with pions in pp collisions at $E_p=0.97$ GeV. A typical result is shown in Fig. 6. The agreement is slightly less good than for the np measurements, but this may be due to the rather poor statistics of the measurements of Ref. [25].

Finally, we also considered the pion data of Ref. [26], using the same ingredients as those of Eqs. (3.1), (3.5), and (3.11). The results are shown in Fig. 7, which clearly demonstrates that the nonisotropic decay of the Δ particles is favored by the comparison of the shape of the spectra, even though the overall pion yield is overestimated by 10 to 15%.[2] Experimental support in favor of the anisotropic decay can also be found in the measurements of Refs. [27,28].

B. Values of the parameters

We consider the parameters $\sigma_{np\to\Delta N}$, $\sigma_{\rm p.s.}$, α and B_{in} successively. We remind the reader that isospin invariance imposes $\sigma_{np\to\Delta^0 p}=\sigma_{np\to\Delta^+ n}$ and that we kept the sum of the first two parameters as

$$\sigma_{np\to\Delta N}+\sigma_{\rm p.s.}=\sigma_{np}^{\rm inel}\,. \tag{4.1}$$

The numerical value of the latter has been taken from Ref. [6]. The quantity $\sigma_{\rm p.s.}$ is found to be given by

$$\frac{\sigma_{\rm p.s.}}{\sigma_{np}^{\rm inel}}=0, \quad p_{\rm lab}<1.6 \ \text{GeV}/c$$
$$=0.262p_{\rm lab}-0.419, \quad p_{\rm lab}>1.6 \ \text{GeV}/c, \tag{4.2}$$

where $p_{\rm lab}$ should be given in GeV/c. The value of this ratio seems to be slightly smaller than the value obtained in Ref. [7], where a similar, but simpler, analysis of their data has been performed. We found that a constant value of $\alpha=6.5(\text{GeV}/c)^{-1}$ is sufficient, in qualitative agreement with the analysis of Ref. [7]. The values of $B_{\rm in}$ yielded by our analysis are given in Fig. 8 along with previously determined

[2]This could indicate that decomposition (3.1) with the chosen parametrization of the inelastic contributions is less valid for the proton-proton case than for the neutron-proton case. However one has to keep in mind that the data shown in Fig. 7 are obtained from extrapolation of measurements performed sometimes on a rather limited range. That is why we did not try to improve the fit on this piece of data.

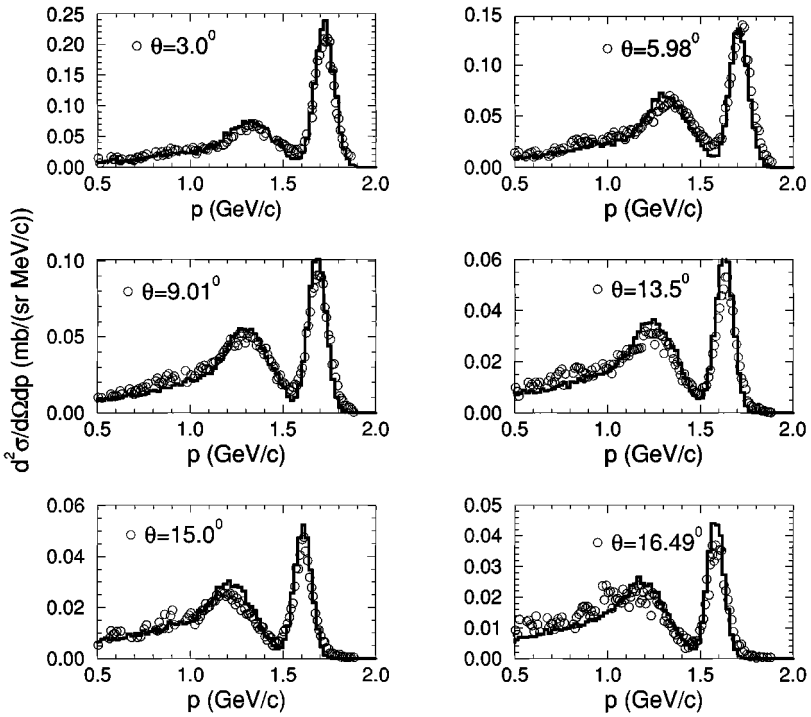

FIG. 5. Momentum spectra of protons emitted at various angles in np collisions at $E_n=1.03$ GeV ($p_{\rm lab}=1.73$ GeV/c), compared to a fit using formula (3.1). The data (symbols) are taken from Ref. [8]. The fit is given by the histograms.

values. A tentative fit to the $p_{\rm lab}$ dependence of all our extracted values is provided by the following form:

$$B_{\rm in}=5.287\left[1+\exp\left(-\frac{p_{\rm lab}-1.3}{0.05}\right)\right]^{-1}, \quad p_{\rm lab}<1.4 \text{ GeV}/c$$
$$=4.65+0.706(p_{\rm lab}-1.4), \quad p_{\rm lab}>1.4 \text{ GeV}/c. \qquad (4.3)$$

This is slightly different from the parametrization proposed in Ref. [6], which rests on a few data only and which is the same as the B-parameter for pp and pn elastic scattering for $p_{\rm lab}\geqslant 1.4$ GeV/c. In particular, the form (4.3) is rising slightly more steeply.

The value of $B_{\rm in}$ for Δ production in pp collisions is not well known. Figure 8 suggests that it may be expected to be similar to the one for the np collisions.

C. Isospin cross sections

As mentioned in Secs. IV A and IV B, formula (3.1) gives a very good representation of the data and can thus be used

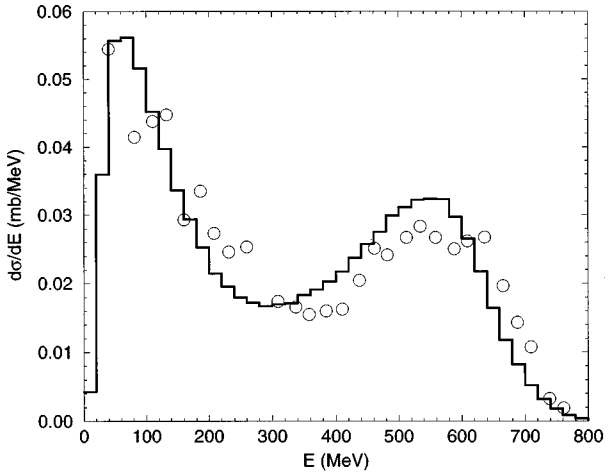

FIG. 6. Energy spectrum of neutrons emitted in pp collisions at $E_p=0.97$ GeV, compared to a fit using formula (3.1). The data (symbols) are taken from Ref. [25]. The fit is given by the histogram.

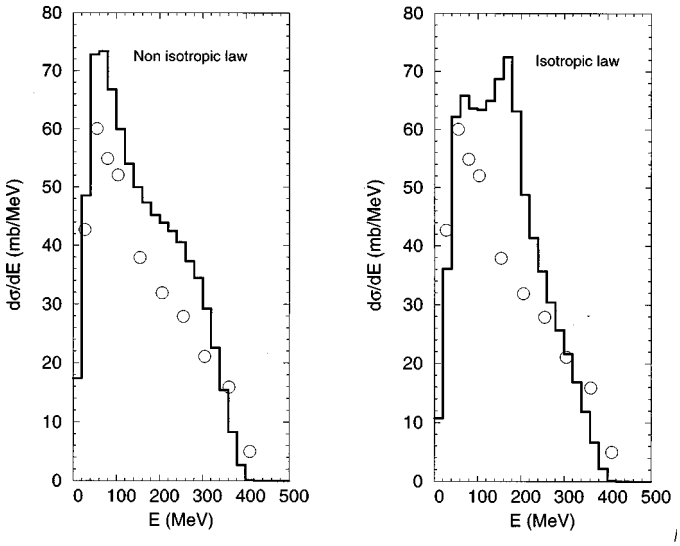

FIG. 7. Energy spectrum of positive pions emitted in pp collisions of 0.73 GeV incident energy compared to fits based on formula (3.1). The data (symbols) are taken from Ref. [26]. The two fits (histograms) correspond to Δ's decaying isotropically (right part) or anisotropically according to the law given by Eq. (3.7).

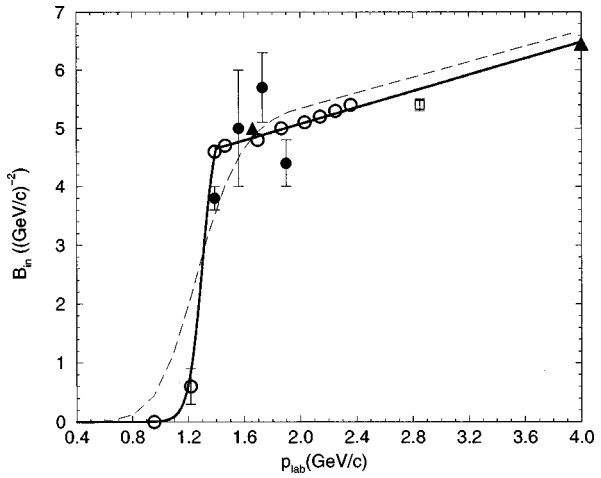

FIG. 8. Values of the slope parameter for the angular distribution of the Δ production in np collisions [see Eq. (3.5)]. The open circles are the results of this work. When not shown explicitly, the error bars on the fitting procedure are less than the size of the symbols. The black circles are given by Ref. [6], which is based on the data of Ref. [7]. The triangle around $p_{\rm lab}\simeq 1.6$ GeV is provided by the present analysis of the pp data of Ref. [25]. The open square corresponds also to the pp system and is taken from Ref. [6]. The triangle at $p_{\rm lab}=4$ GeV/c is taken from Ref. [32]. The full line is a simple fit of the data. Its shape is given by Eq. (4.3). The dashed line is extracted from Ref. [6].

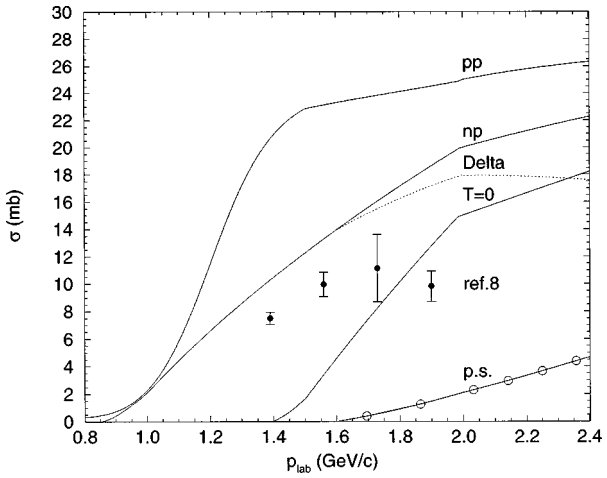

FIG. 9. The full lines give the total inelastic pp and np cross sections as parametrized in Ref. [6] and the $T=0$ NN cross section, obtained from Eq. (4.4) and these parametrizations. The dotted line gives the $np\rightarrow\Delta+X$ cross section provided by the present analysis. The black dots are the values of the same cross section given by Ref. [8], assuming isospin symmetry and a symmetric Δ mass distribution. The curve joining the open circles represents the quantity $\sigma_{\rm p.s.}$ defined in Eq. (3.12) and extracted from the present analysis.

directly as input for transport calculations. The question arises to know whether it provides a faithful and practical representation of the data or whether the various terms of this formula have a well defined physical meaning. Of course, this question does not refer to the elastic contribution, but to the inelastic terms, as the parametrization of the latter are based on some hypotheses. One may wonder for instance whether the term which we call ''Δ production'' does really give the importance of the formation of a physical Δ. For this to be true, the extracted value of this contribution should be consistent with the constraint imposed by isospin symmetry. This is the subject of this section.

The total inelastic np cross section is the average of the isospin $T=1$ and $T=0$ inelastic cross sections. The latter can be obtained through the relations

$$\sigma_{NN,\rm inel}^{T=0}=2\sigma_{np}^{\rm inel}-\sigma_{pp}^{\rm inel}, \quad \sigma_{NN,\rm inel}^{T=1}=\sigma_{pp}^{\rm inel}. \tag{4.4}$$

They are given in Fig. 9, using the parametrization of Ref. [6] for the empirical pp and np total inelastic cross sections (for the sake of clarity, a small bump of ~ 3 mb in $\sigma_{NN,\rm inel}^{T=0}$ around $p_{\rm lab}\sim 1.1$ GeV/c is not shown). The numerical values of $\sigma_{NN,\rm inel}^{T=0}$ are very similar to those given in Ref. [5], although they are smaller by $\sim 25\%$ around 1.6 GeV/c. This seems to be due to the dispersion of the available data for some of the inelastic channels (in particular the $np\pi_0$ channel) in this range, which allow somewhat different but equally acceptable parametrizations of $\sigma_{np}^{\rm inel}$ and $\sigma_{pp}^{\rm inel}$. In any case, below $p_{\rm lab}\approx 1.6$ GeV/c, the $T=0$ cross section is small and the interpretation of the inelastic scattering, proceeding basically through the $T=1$ channel, as due to Δ production only is legitimate. Above this value, this assignment becomes questionable (even though the fit is good), as the ''direct'' pion production ($\sigma^{\rm p.s.}$), which could be a $T=0$ process, does not exhaust the indicated $T=0$ cross section (see Fig. 9). Note, however, that the experimental situation is not so clear; there is some apparent ''violation'' of isospin symmetry in the available one pion production data [5]. Since assumptions based on that symmetry have to be made in order to sum over all partial inelastic channels, this inevitably influences in one way or the other the estimated total inelastic cross section. It seems anyway that, in spite of these uncertainties, there are good reasons [5,29] to believe that the $T=0$ channel is basically elastic below ~ 1.6 GeV/c. Above this value, the situation is uncertain. The careful investigation of Bystricky *et al.* [5] shows that the $T=0$ pion production cross section could grow linearly from basically zero at $p_{\rm lab}=1.6$ GeV/c to reach ~ 8 mb at $p_{\rm lab}=2.35$ GeV/c ($E_n=1.6$ GeV), not so much larger than our $\sigma_{\rm p.s.}$. Summarizing this discussion, we can state that there is no inconsistency, with respect to isospin symmetry, in our determination of the Δ-production cross section below ~ 1.6 GeV/c. Above this value the numbers extracted from our procedure cannot be more accurate than the difference between the smallest estimate of the $T=0$ cross section and $\sigma_{\rm p.s.}$, which amounts to $\sim 20\%$ at ~ 2.2 GeV/c. Nevertheless, our parametrization keeps the property of providing a good representation of the data.

V. DISCUSSION AND CONCLUSION

The three term formula (3.1) that we used to analyze proton spectra embodies elastic scattering, production through Δ resonances and ''direct'' production. The Δ-production term is inspired from a classical model, which considers the intermediate Δ resonance as a classical particle with a definite mass, determined stochastically event by event, according to distribution (3.6). This procedure is basically the same as the one adopted in most transport models to handle interactions

of the intermediate Δ with other particles in complex p-nucleus or heavy ion collisions. However, Eq. (3.5) bears some similarity with the results of one pion exchange models, as we have indicated in Sec. III. We have neglected two pion production, which indeed is vanishingly small below 1 GeV, but whose importance may correspond to a cross section of a few mb at 1.6 GeV. All the assumptions introduced by Eqs. (3.1)–(3.11) are quite reasonable, except perhaps at the largest energies investigated here.

One of our main results is the determination of the parameter $B_{\rm in}$ (Fig. 8). The data of Ref. [9] being limited to small angles do not probe a large domain of t. They alone do not constraint the parameter $B_{\rm in}$ very much, but rather the product $\sigma_{np\to\Delta}B_{\rm in}$ [see Eqs. (3.5) and (3.9)]. The data of Ref. [8] extending to much larger angles constrain $B_{\rm in}$ more efficiently. Note that the cross section falls down by a factor 4 or so over the range of accessible values of t. It is interesting to note that the values of $B_{\rm in}$ appear to be close to those of the slope parameter for pp elastic scattering and to those of pn elastic scattering for $p_{\rm lab}$ larger than $\sim$1.4 GeV/c. The large values of $B_{\rm in}$ in this range confirms the peripheral nature of Δ production.

The parameters $\sigma_{\rm p.s.}$ and α are rather well determined by the fitting procedure. However their physical meaning remains unclear. There is a definite need to introduce a component besides the Δ production. Otherwise, the yield is underestimated at low proton momemtum, for $p_{\rm lab}$ larger than $\sim$1.6 GeV/c. This necessary contribution could originate from several physical processes: (i) double pion production. One pion exchange models predict a small contribution from this process in the kinematical range under investigation, although, experimentally, the total cross section for these channels is rising sizably above 1.6 GeV/c. (ii) Excitation of the Roper resonance, the missing yield being situated just at the corresponding kinematics. (iii) Genuine direct one pion production, as we have assumed. (iv) Final state interaction between the detected nucleon and the decay products of the resonance. The second possibility is very appealing. We have fitted the 1.6 GeV data quite well with a second resonance having an average mass of $\sim$1.5 GeV and a width of $\sim$0.15 GeV, but the required cross section amounts to $\sim$40% of the total inelastic cross section, which looks unrealistic for the Roper resonance. Presumably, the physical situation corresponds to a mixture of effects (ii) and (iii) above. The limited amount of data does not allow to discrimate among the various possibilities.

Assuming Δ production as the dominant process biases the analysis in favor of a $T=1$ dominance. We note however that the experimental information on pp and np total inelastic cross section justifies this assumption for $E_n \lesssim 1$ GeV. Additional support of this line of approach is provided by the fact that we observe the same B_{in} for np and pp (when the latter is available) and by the quality of the fit itself. Let us finally mention that fitting low energy data with the total inelastic cross section is rather surprising, as close to threshold the $np\to d\pi^0$ process dominates. However this process extinguishes rather quickly and the cross-section never exceeds 1.5 mb.

In conclusion, we have proposed a representation of the inelastic nucleon-nucleon cross-section below $\sim$1.6 GeV and we have determined its parameters with a good accuracy. We did not attempt to a χ^2 fit, but proceeded through visual evaluation of the quality of the fit. That convinces us nevertheless that the parameters are determined with an accuracy sufficient to be used as data for transport calculations, i.e., with an accuracy better than, say, 10%. We want to warn however the casual reader who would require a much better accuracy, of the order of one percent, for instance. We have also shown that the $np\to\Delta N$ cross section can be identified with the (second) ''resonant'' term of our parametrization (3.1) for incident energy up to $\sim$1 GeV. Above this value, this identification is less and less reliable and the discrepancy may reach $\sim$20% at $E_n=1.6$ GeV, although the accuracy of the whole parametrization remains the same. We have also determined the slope parameter $B_{\rm in}$ with good accuracy in the 0.6–1.6 GeV range, improving considerably the phenomenological knowledge of this quantity. Parameters related to the ''phase space'' contribution are numerically determined with good accuracy, but do not have an obvious physical meaning. Let us finally notice that model descriptions of proton induced spallation reactions up to 1 GeV, which recently received a renewed interest in relation with the so-called hybrid systems [30,31], can safely be pursed with the inelasticity restricted to the Δ production channel. They can benefit from the results obtained in this work.

[1] J. Cugnon, Nucl. Phys. **A462**, 751 (1987).

[2] J. Aichelin, Phys. Rep. **202C**, 233 (1991).

[3] A. Baldini, V. Flaminio, W.G. Moorhead, and D.R.O. Morrison, in *Total Cross-Sections for Reactions of High Energy Particles (including Exchange, Elastic, Topological, Inclusive and Exclusive Reactions)*, edited by H. Schopper, Landolt-Börnstein, New Series, Group I, Vol. 12a (Springer-Verlag, Berlin, 1988).

[4] J. Bystricky, C. Lechanoine-Leluc, and F. Lehar, J. Phys. (France) **48**, 199 (1987).

[5] J. Bystricky, P. La France, F. Lehar, F. Perrot, T. Siemiarczuk, and P. Winternitz, J. Phys. (France) **48**, 1901 (1987).

[6] J. Cugnon, D. L'Hôte, and J. Vandermeulen, Nucl. Instrum. Methods Phys. Res. B **111**, 215 (1996).

[7] J.L. Laville, PhD. thesis, University of Caen, 1976.

[8] G. Bizard *et al.*, Nucl. Phys. **B108**, 189 (1976).

[9] E. Martinez *et al.*, Nucl. Instrum. Methods Phys. Res. A **385**, 345 (1997).

[10] G. Bizard *et al.*, Nucl. Instrum. Methods **111**, 451 (1973).

[11] R.A. Arndt, I.I. Strakovsky, and R.L. Workman, Phys. Rev. C **50**, 2731 (1994) and Interactive Dial-in Program SAID, FA95 solution.

[12] R.K. Keller *et al.*, Nucl. Phys. **A377**, 543 (1982).

[13] A.J. Becsbuch *et al.*, Phys. Rev. D **13**, 535 (1976).

[14] A.J. Hertzler *et al.*, Phys. Rev. **95**, 591 (1954).

[15] L.C. Northcliffe *et al.*, Phys. Rev. C **47**, 36 (1993).

[16] R. Silverman *et al.*, Nucl. Phys. **A499**, 763 (1989).
[17] M.L. Evans *et al.*, Phys. Rev. C **26**, 2525 (1982).
[18] M. Jain *et al.*, Phys. Rev. C **30**, 566 (1984).
[19] G. Bizard *et al.*, Nucl. Phys. **B85**, 14 (1975).
[20] Y. Terrien *et al.*, Phys. Rev. Lett. **59**, 1534 (1987).
[21] G.F. Chew, Phys. Rev. **112**, 1380 (1958).
[22] H.W. Bertini *et al.*, Phys. Rev. **131**, 1801 (1963).
[23] E. Ferrari and F. Selleri, Nuovo Cimento **XXVII**, (6), 1450 (1963).
[24] J. Cugnon, T. Mizutani, and J. Vandermeulen, Nucl. Phys. **A352**, 505 (1981).
[25] D. Bugg *et al.*, Phys. Rev. **133B**, 1017 (1964).
[26] D.R.F. Cochran *et al.*, Phys. Rev. D **6**, 3085 (1972).
[27] K.L. Wolff *et al.*, Phys. Rev. Lett. **42**, 1448 (1979).
[28] K. Nakai *et al.*, Phys. Rev. C **20**, 2210 (1979).
[29] B.J. Verwest and R.A. Arndt, Phys. Rev. C **25**, 1979 (1982).
[30] C.D. Bowman *et al.*, Nucl. Instrum. Methods Phys. Res. A **320**, 336 (1992).
[31] C. Rubbia *et al.*, ''Conceptual design of a fast neutron operated high power energy amplifier,'' Report No. CERN/AT/95-44(ET), 1995.
[32] S. Coletti *et al.*, Nuovo Cimento A **49**, 479 (1967).